L-299

NATIONAL ADVISORY COMMITTEE FOR AERONAUTICS

WARTIME REPORT

ORIGINALLY ISSUED
November 1943 as
Advance Confidential Report 3K13

LIFT AND DRAG DATA FOR 30 PUSHER-PROPELLER SHAFT HOUSINGS ON AN NACA 65,3-018 AIRFOIL SECTION

By Frank T. Abbott, Jr.

Langley Memorial Aeronautical Laboratory
Langley Field, Va.

NACA

WASHINGTON

NACA WARTIME REPORTS are reprints of papers originally issued to provide rapid distribution of advance research results to an authorized group requiring them for the war effort. They were previously held under a security status but are now unclassified. Some of these reports were not technically edited. All have been reproduced without change in order to expedite general distribution.

NATIONAL ADVISORY COMMITTEE FOR AERONAUTICS

ADVANCE CONFIDENTAL REPORT

LIFT AND DRAG DATA FOR 30 PUSHER-PROPELLER SHAFT HOUSINGS ON AN NACA 65,3-018 AIRFOIL SECTION

By Frank T. Abbott, Jr.

SUMMARY

Tests were made in the NACA two-dimensional low-turbulence pressure tunnel to study the interference effects of various pusher-propeller shaft-housing combinations on an NACA low-drag airfoil. Thirty different combinations were tested, variations being made in shaft size, shape, angle, and fillet. The shafts were not equipped with operating propellers. Results of this study indicated that drag increments increased roughly in proportion to shaft diameter, that increasing the shaft angle caused large increases in the drag increments, that fillets should be small but not abruptly ended, and that the combinations with shaft angles greater than 0° caused a slight decrease in lift.

INTRODUCTION

As part of a general program of investigation of interference effects on low-drag wings, studies have been made of the effects of leading-edge roughness, intersecting flat plates, and nacelles (references 1 to 4). These studies have shown that the largest adverse effects are caused by leading-edge roughness. Other sources of interference have, in general, failed to show large adverse interference effects on drag except the drag increment resulting directly from a more forward location of transition from laminar to turbulent flow. These results would indicate that no serious adverse interference effects would be expected from pusher-propeller shaft housings on low-drag wings.

Tests in the NACA 19-foot pressure tunnel of a model of the XB-35 airplane (unpublished), however, showed unexpectedly large drag increments due to the pusher-propeller

shaft housings. Because the model had large sweepback, the question arose as to whether the drag increment largely resulted from cross flows due to the sweepback or from the shape of the propeller shaft housing itself. It was therefore decided to test a similar propeller shaft housing on an airfoil model in the NACA two-dimensional low-turbulence pressure tunnel to investigate the drag without sweepback. Tests were made and the results were found to be about the same as those obtained in the NACA 19-foot pressure tunnel. These results indicated that the drag increments could not be attributed primarily to cross flows resulting from sweepback.

Because the number of applications of pusher propellers on new airplanes is increasing, it was decided to extend the investigation to include other combinations. A series of tests has been made of 30 different combinations varying in shaft shape, size, angle, and fillet. These shafts were not equipped with operating propellers. Although it was realized that operating propellers would affect the results obtained, it was thought that the chief result would be to improve the poorer combinations. Further tests of some of these shaft and fillet combinations with propellers operating are planned.

MODEL

A 24-inch-chord model having an NACA 65,3-018 airfoil section (reference 1) was used for all the tests. This model was made of wood with painted and sanded surfaces and extended from wall to wall of the rectangular test section of the NACA two-dimensional low-turbulence pressure tunnel. The pusher shaft housings were also made of wood with surfaces painted and sanded and the fillets were made of modeling clay. Each arrangement was mounted on the wing at about the center of the span, as shown in figure 1. Three sizes of shaft housings were tested and are referred to as the small (0.07c), medium (0.11c), and large (0.15c) shafts. Each of these shafts was tested at various angles to the wing chord line. As shown in figure 2, the center lines of all shafts intersected the wing chord line at the same point, and the lengths of the shafts were the same regardless of size or angle. A short (0.14c) and a long (0.21c) spinner were tested on the small shaft. Spinners on the medium and large shafts were proportioned to correspond to the short spinner on the small shaft. The arrangements are all illustrated by sketches (figs. 3 to 32), which are drawn to scale. General dimensions for all the arrangements are shown in figure 2.

For several tests, the small and medium shafts at the 10° angle were reduced in width to about two-thirds the diameter of the corresponding round shaft over a part of their lengths, and an attempt was made to streamline this reduced portion to the local air flow. (See figs. 10 to 14 and 20.) The spinners, of course, remained round. The shafts in this condition will be referred to as streamline.

The medium shaft was also tested in another condition in which the shaft cross sections remained round but the diameter varied from about two-thirds of the full diameter at the point of intersection with the wing to full diameter at the beginning of the spinner. (See figs. 23 and 24.) The shaft in this condition will be referred to as tapered.

METHODS

Lift data were obtained by measurement of the reaction of the model on the floor and the ceiling of the wind tunnel, as described in reference 1. The model lift coefficient c_l based on the model area of 6 square feet is used in the presentation of the lift data.

Drag measurements were made at lift coefficients from about 0.2 to 0.5 by the wake-survey method at a number of spanwise points. The drag values obtained were plotted against distance along the span of the model and drag-coefficient increments were obtained by integrating the resulting diagrams. The drag-coefficient increments are given for each combination in tabular form on figures 3 to 32 as ΔC_{D_1} and ΔC_{D_2}. These increments are the total-drag increments of the shaft housings, that is, the external-drag increments plus the interference-drag increments.

The values designated ΔC_{D_1} are the additional drag increments caused by four installations at a chord of 344 inches and based on a wing area of 4000 square feet. These dimensions correspond approximately to those of the XB-35 airplane. The drag increments designated ΔC_{D_2} are for a single installation based on an area equal to 1 chord length of span (the chord squared).

In regard to the accuracy of the drag increments given, it should be noted that the measurements were made by the wake-survey method. Although this method is very accurate for two-dimensional flow, it has been observed in other tests of a different nature that, where strong localized vortices are present in the flow, the wake-survey method may

fail to measure all the drag even when the survey is made over a distance considerably wider than the region producing the vortex. It is thought that this condition was present only to a small extent in these tests.

All the tests were made at a wing Reynolds number R of about 6,000,000.

RESULTS AND DISCUSSION

Effects of Shaft Size

Drag increments increased considerably with shaft size, as shown by figure 33. At some shaft angles, with the best fillets, the drag increments were roughly in proportion to the diameter of the shaft (fig. 33). Although the large shafts gave higher drag increments than the small shafts, their use may be desirable on some airplanes to improve propeller characteristics by permitting the enclosure of thick root sections within the spinner.

Effects of Spinner Length

Lengthening the spinner of the small shaft, as shown in figures 12, 13, and 18, gave a slight reduction in drag increments from the corresponding conditions with the short spinner. Although longer spinners were not tested on the medium and large shafts, it is probable that similar results would have been found.

Effects of Shaft Angle

Shaft angle had a large effect on the drag characteristics of all three shafts, as shown in figure 33. Each reduction of shaft angle brought about a reduction of the drag increments. For example, the drag increments for the small round shaft at an angle of 3.25° were only about one-third as large as those for the shaft at 10°.

Effects of Shaft and Fillet Shape

Most of the variations in shaft and fillet shape were made with the small shaft at an angle of 10°. The best fillet shape tested for this condition is shown in figure 8.

As shown by the sketch, this fillet was small and slender and had a fairly high fineness ratio. It is apparent from the results for the other arrangements that there is an optimum size for such a fillet. Large flaring fillets (fig. 4), excessively long ones (fig. 7), and very short blunt-tail ones (fig. 9) caused unnecessarily high drag increments. Fairings in addition to fillets such as those shown in figures 5 and 14 caused an increase in drag increments.

Variations in fillet shape for the other shaft conditions were minor and usually failed to show much change in drag with fillet shape. For both the medium shaft (figs. 25 and 26) and the large shaft (figs. 31 and 32) at an angle of 0°, the very small fillets gave drag increments as low as those of the larger fillets.

Streamlining the small and medium shafts at the 10° angle, as shown in figures 10, 11, and 20, had very little effect on drag characteristics. Tapering the medium shaft, as shown in figures 23 and 24, likewise had very little effect on the drag.

Effects on Lift Characteristics

Figure 34 shows the lift characteristics of four typical combinations compared with the plain wing. This figure shows that, when the shaft angle is greater than 0°, a slight decrease in lift coefficient occurs at the smaller angles of attack and at maximum lift. This decrease in lift coefficient at the smaller angles of attack is caused principally by a slight increase in the angle of zero lift with very little change in the lift-curve slope. When the shaft angle is 0°, the lift coefficients are approximately the same as those of the plain wing except in the region near maximum lift.

CONCLUSIONS

For the conditions tested, the study of 30 pusher-propeller shaft housings on an NACA 65,3-018 airfoil section indicated that:

1. Drag increments increased with shaft size somewhat in proportion to the diameter of the shaft for any given angle tested.

2. Drag increments increased rapidly as the angle between the shaft and the wing chord line increased.

3. For shaft arrangements of the type tested, the lowest drag increments were obtained with small slender fillets having fairly high fineness ratios. Large flaring fillets, excessively long ones, and short blunt-tail ones should be avoided, especially at the higher shaft angles.

4. All of the shaft combinations with shaft angles greater than 0° caused slight decreases in lift coefficient. When the shaft angle was 0°, practically no decrease in lift coefficient occurred.

Langley Memorial Aeronautical Laboratory,
National Advisory Committee for Aeronautics,
Langley Field, Va.

REFERENCES

1. Jacobs, Eastman N., Abbott, Ira H., and Davidson, Milton: Preliminary Low-Drag-Airfoil and Flap Data from Tests at Large Reynolds Numbers and Low Turbulence, and Supplement. NACA ACR, March 1942.

2. Jacobs, Eastman N., Abbott, Ira H., and Davidson, Milton: Investigation of Extreme Leading-Edge Roughness on Thick Low-Drag Airfoils to Indicate Those Critical to Separation. NACA CB, June 1942.

3. Abbott, Ira H.: Interference Effects of Longitudinal Flat Plates on Low-Drag Airfoils. NACA CB, Nov. 1942.

4. Ellis, Macon C., Jr.: Effects of a Typical Nacelle on the Characteristics of a Thick Low-Drag Airfoil Critically Affected by Leading-Edge Roughness. NACA CB No. 3D27, April 1943.

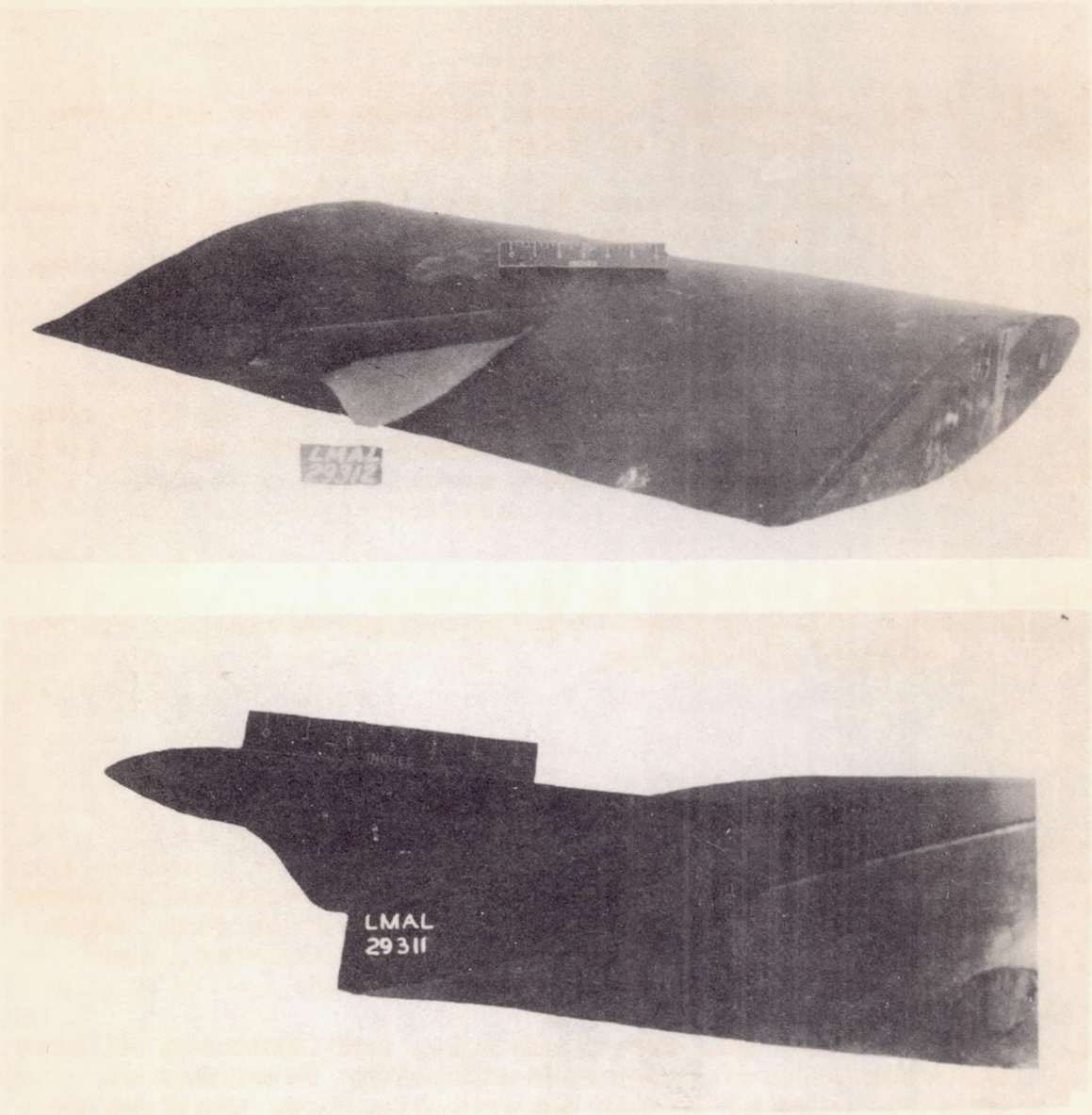

Figure 1. - NACA 65,3-018 airfoil section model with pusher-propeller shaft; fillet A; β, 10°; a, 0.1392c; b, 0.0729c. (See figs. 2 and 3.)

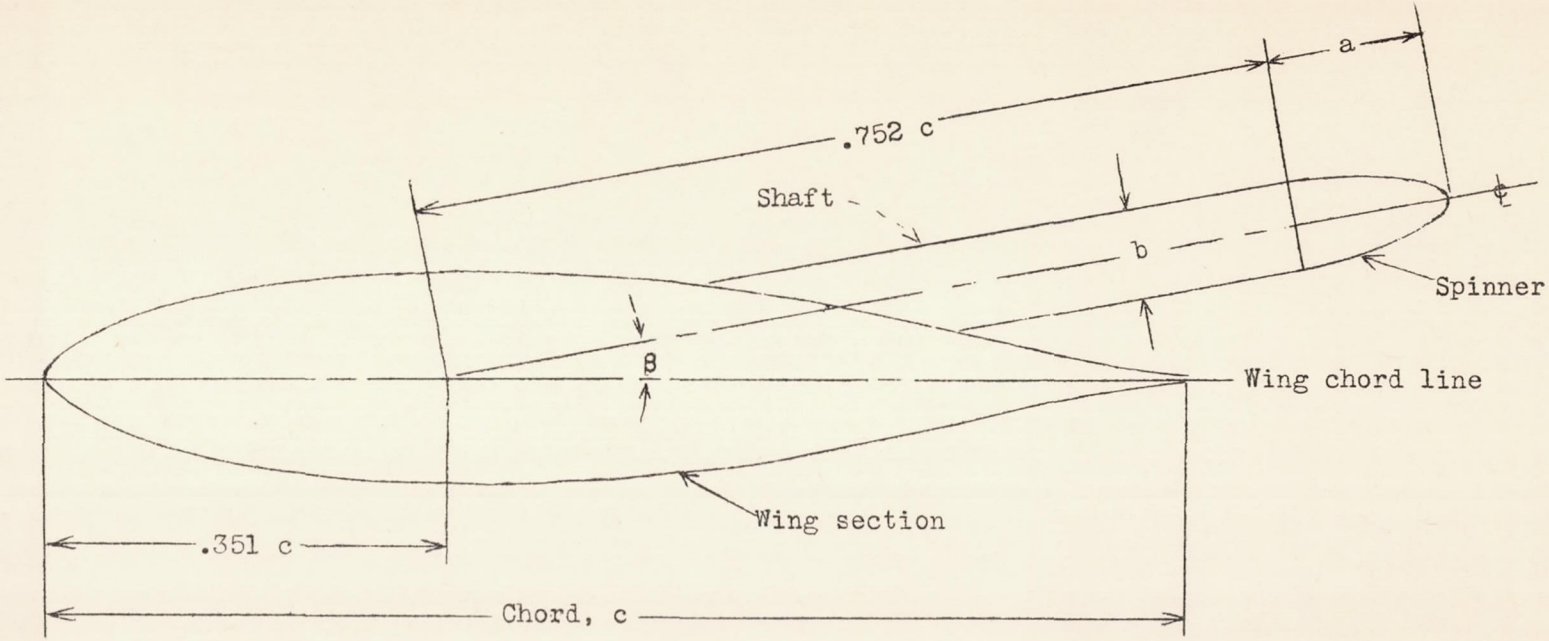

Figure 2.-General dimensions for sketches of pusher propeller shaft housings on NACA 65,3-018 airfoil.

L-299

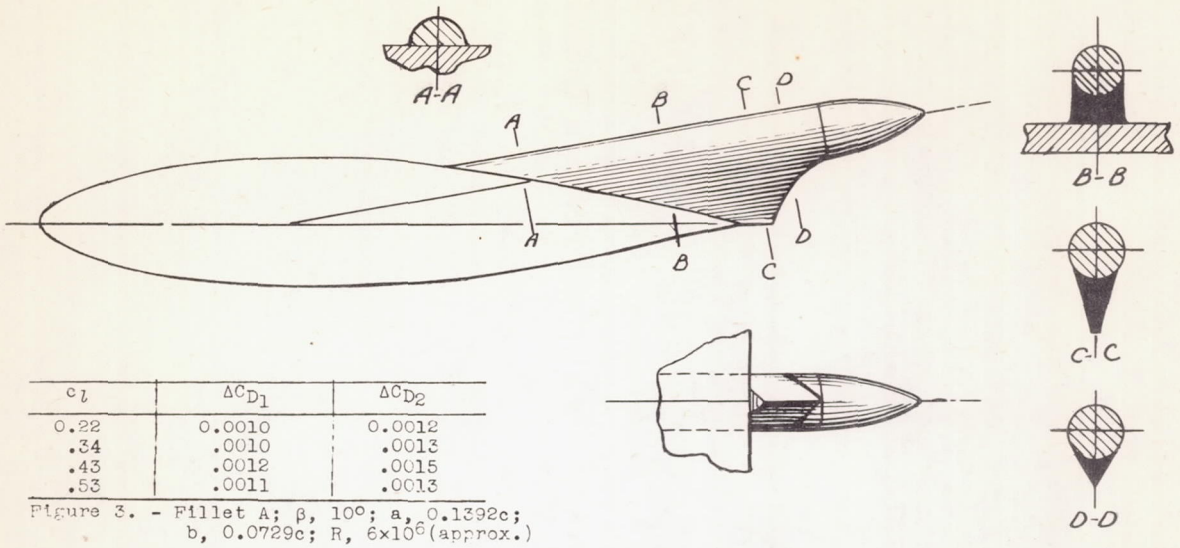

c_l	ΔC_{D_1}	ΔC_{D_2}
0.22	0.0010	0.0012
.34	.0010	.0013
.43	.0012	.0015
.53	.0011	.0013

Figure 3. - Fillet A; β, 10°; a, 0.1392c; b, 0.0729c; R, 6×10^6 (approx.)

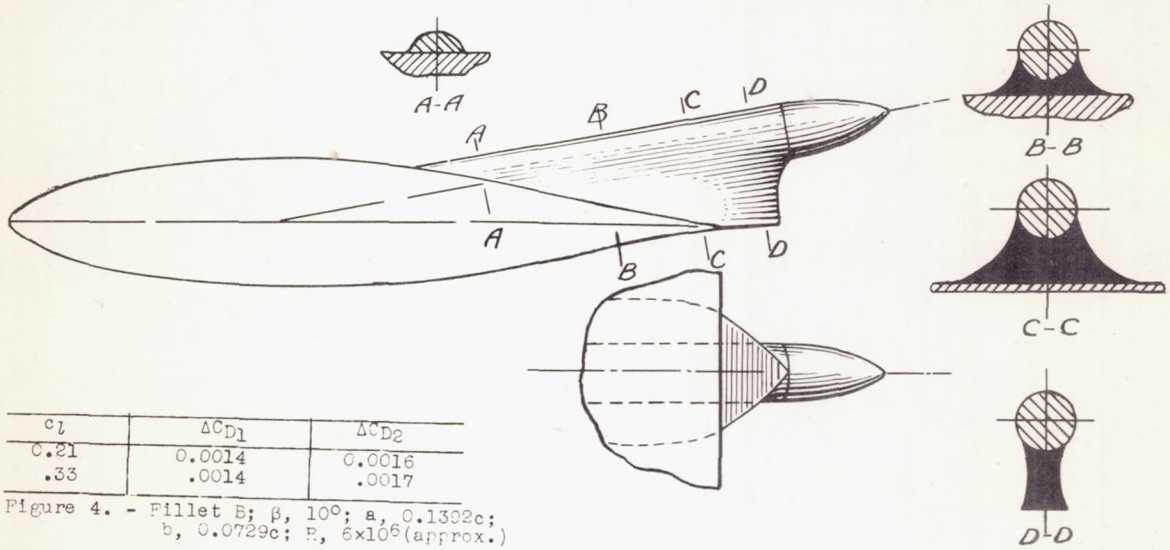

c_l	ΔC_{D_1}	ΔC_{D_2}
0.21	0.0014	0.0016
.33	.0014	.0017

Figure 4. - Fillet B; β, 10°; a, 0.1392c; b, 0.0729c; R, 6×10^6 (approx.)

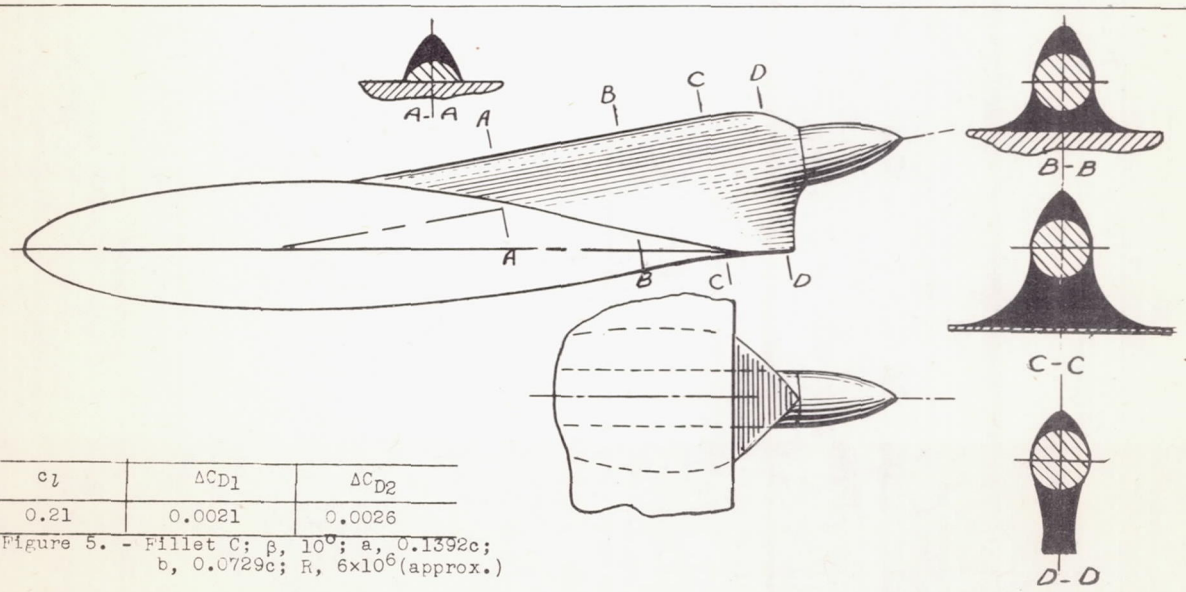

c_l	ΔC_{D_1}	ΔC_{D_2}
0.21	0.0021	0.0026

Figure 5. - Fillet C; β, 10°; a, 0.1392c; b, 0.0729c; R, 6×10^6 (approx.)

L-299

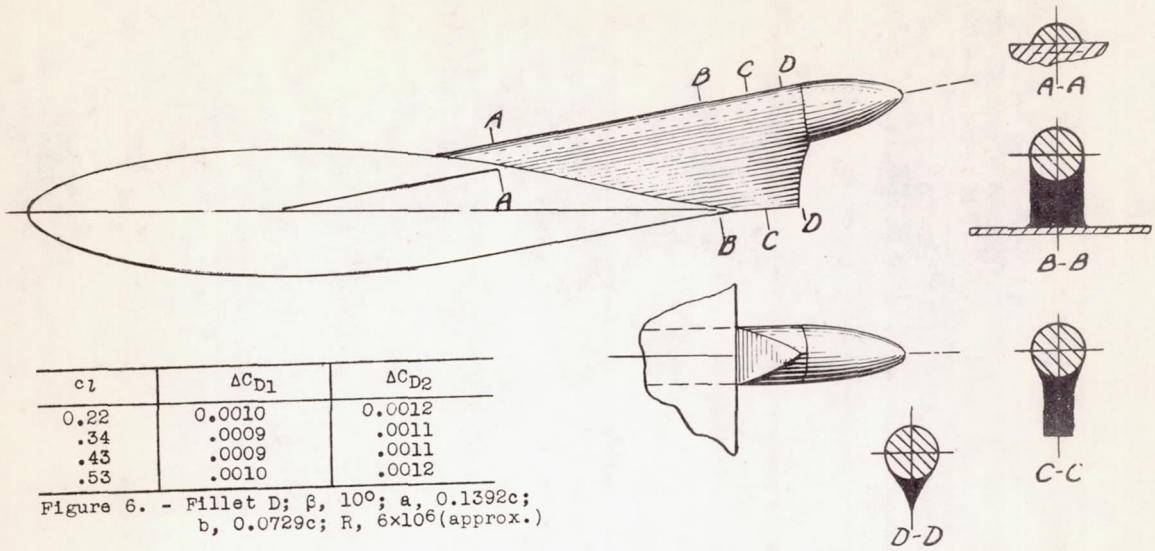

c_l	ΔC_{D1}	ΔC_{D2}
0.22	0.0010	0.0012
.34	.0009	.0011
.43	.0009	.0011
.53	.0010	.0012

Figure 6. - Fillet D; β, 10°; a, 0.1392c; b, 0.0729c; R, 6×10^6(approx.)

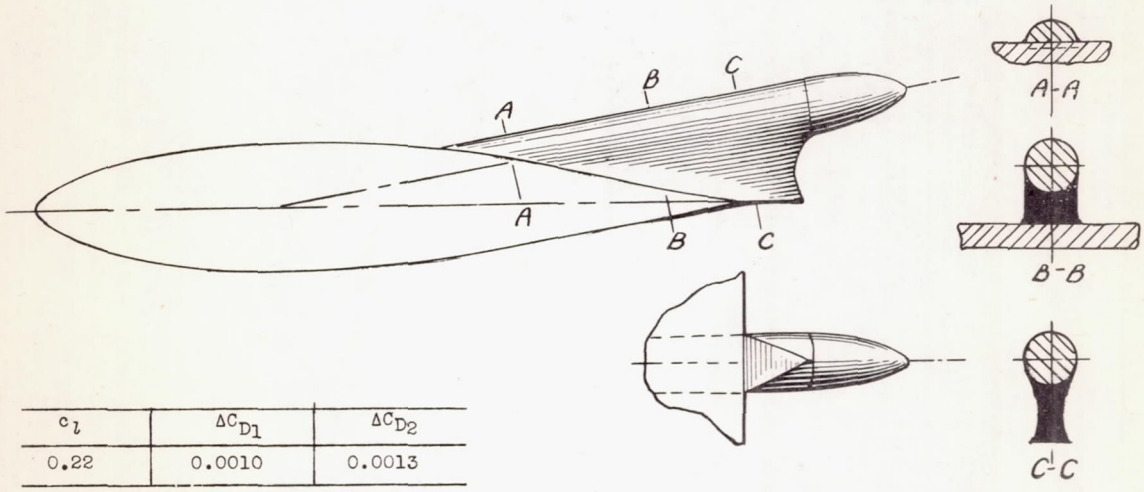

c_l	ΔC_{D1}	ΔC_{D2}
0.22	0.0010	0.0013

Figure 7. - Fillet E; β, 10°; a, 0.1392c; b, 0.0729c; R, 6×10^6(approx.)

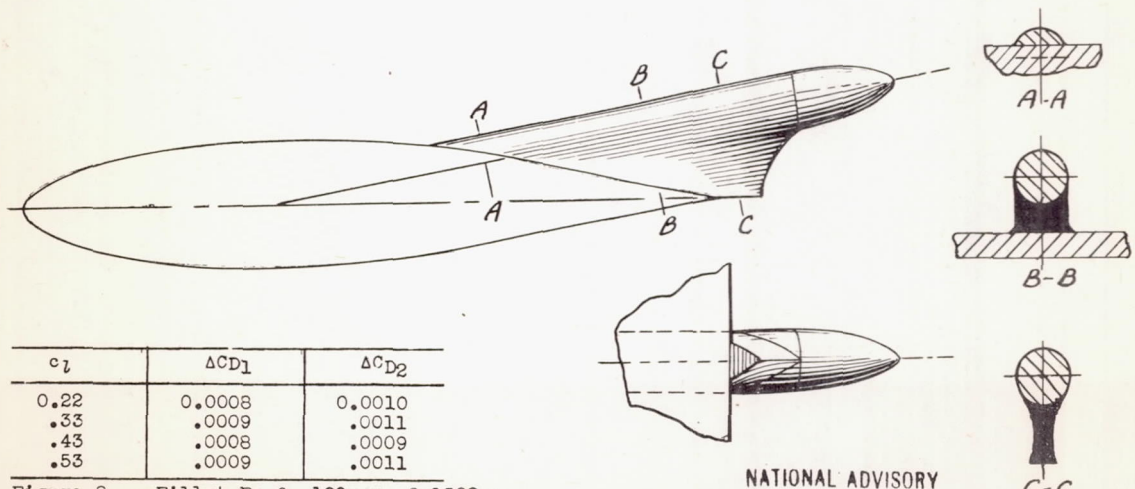

c_l	ΔC_{D1}	ΔC_{D2}
0.22	0.0008	0.0010
.33	.0009	.0011
.43	.0008	.0009
.53	.0009	.0011

Figure 8. - Fillet F; β, 10°; a, 0.1392c; b, 0.0729c; R, 6×10^6(approx.)

NATIONAL ADVISORY COMMITTEE FOR AERONAUTICS

L-299

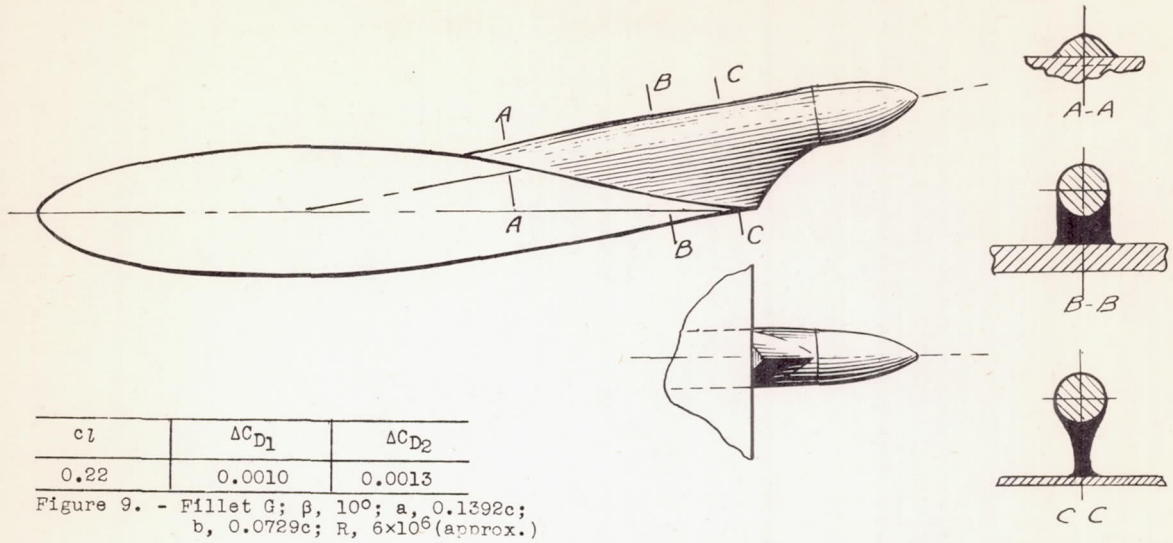

c_l	ΔC_{D_1}	ΔC_{D_2}
0.22	0.0010	0.0013

Figure 9. - Fillet G; β, 10°; a, 0.1392c; b, 0.0729c; R, 6×10^6 (approx.)

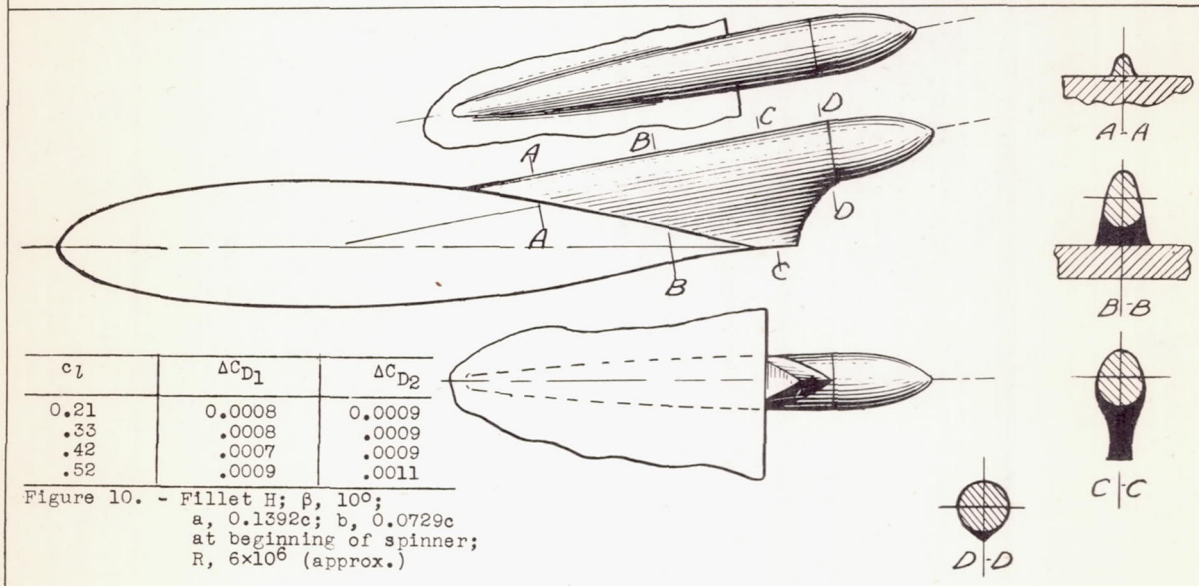

c_l	ΔC_{D_1}	ΔC_{D_2}
0.21	0.0008	0.0009
.33	.0008	.0009
.42	.0007	.0009
.52	.0009	.0011

Figure 10. - Fillet H; β, 10°; a, 0.1392c; b, 0.0729c at beginning of spinner; R, 6×10^6 (approx.)

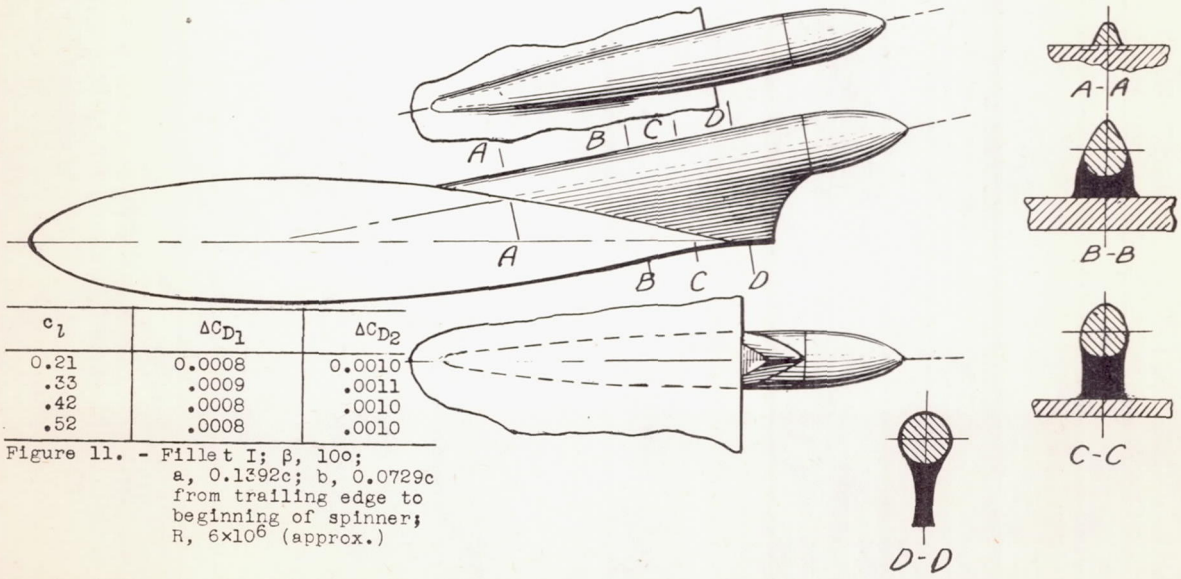

c_l	ΔC_{D_1}	ΔC_{D_2}
0.21	0.0008	0.0010
.33	.0009	.0011
.42	.0008	.0010
.52	.0008	.0010

Figure 11. - Fillet I; β, 10°; a, 0.1392c; b, 0.0729c from trailing edge to beginning of spinner; R, 6×10^6 (approx.)

L-299

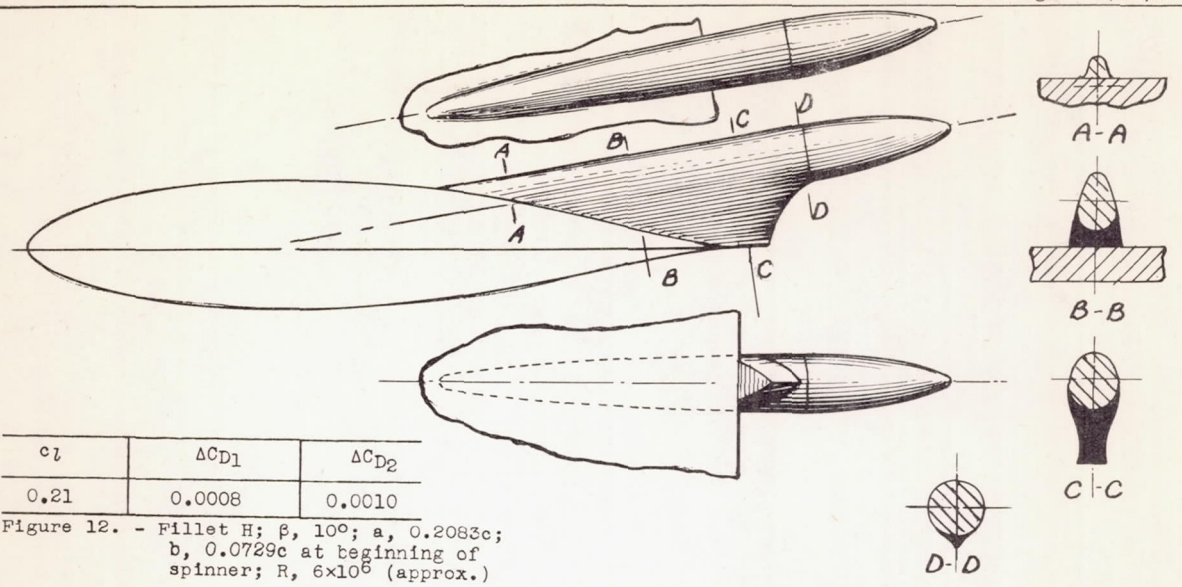

c_l	ΔC_{D_1}	ΔC_{D_2}
0.21	0.0008	0.0010

Figure 12. - Fillet H; β, 10°; a, 0.2083c; b, 0.0729c at beginning of spinner; R, 6×10^6 (approx.)

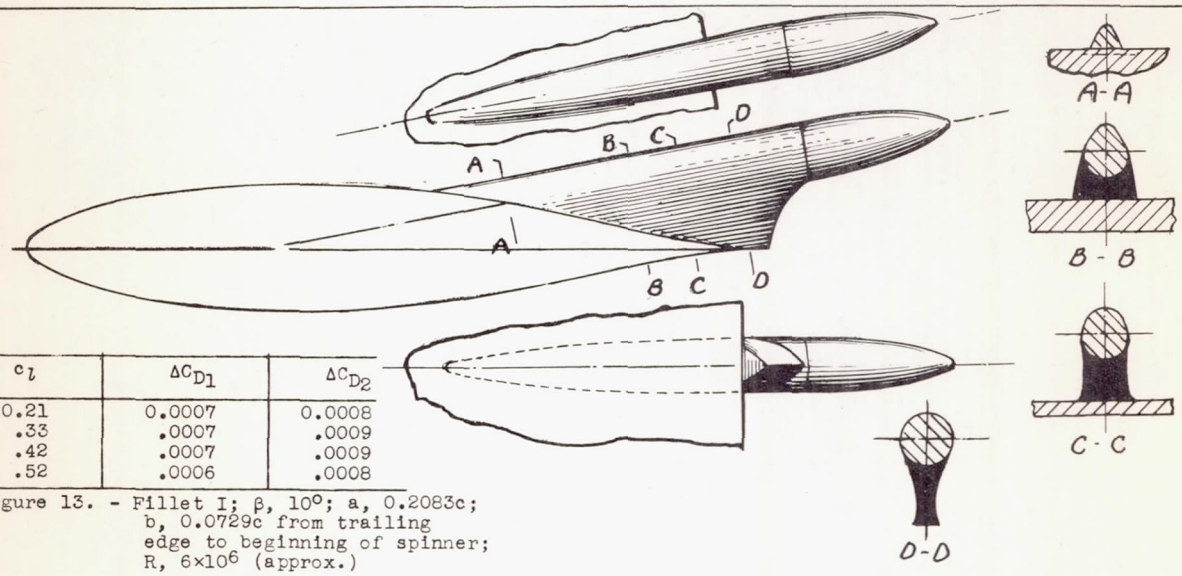

c_l	ΔC_{D_1}	ΔC_{D_2}
0.21	0.0007	0.0008
.33	.0007	.0009
.42	.0007	.0009
.52	.0006	.0008

Figure 13. - Fillet I; β, 10°; a, 0.2083c; b, 0.0729c from trailing edge to beginning of spinner; R, 6×10^6 (approx.)

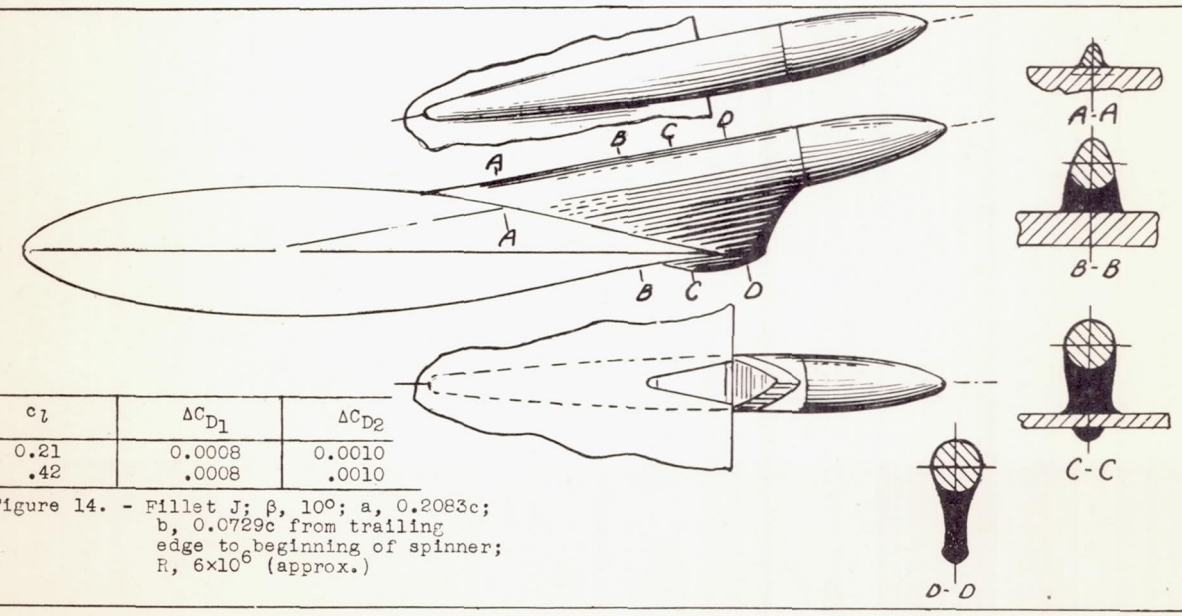

c_l	ΔC_{D_1}	ΔC_{D_2}
0.21	0.0008	0.0010
.42	.0008	.0010

Figure 14. - Fillet J; β, 10°; a, 0.2083c; b, 0.0729c from trailing edge to beginning of spinner; R, 6×10^6 (approx.)

L-299

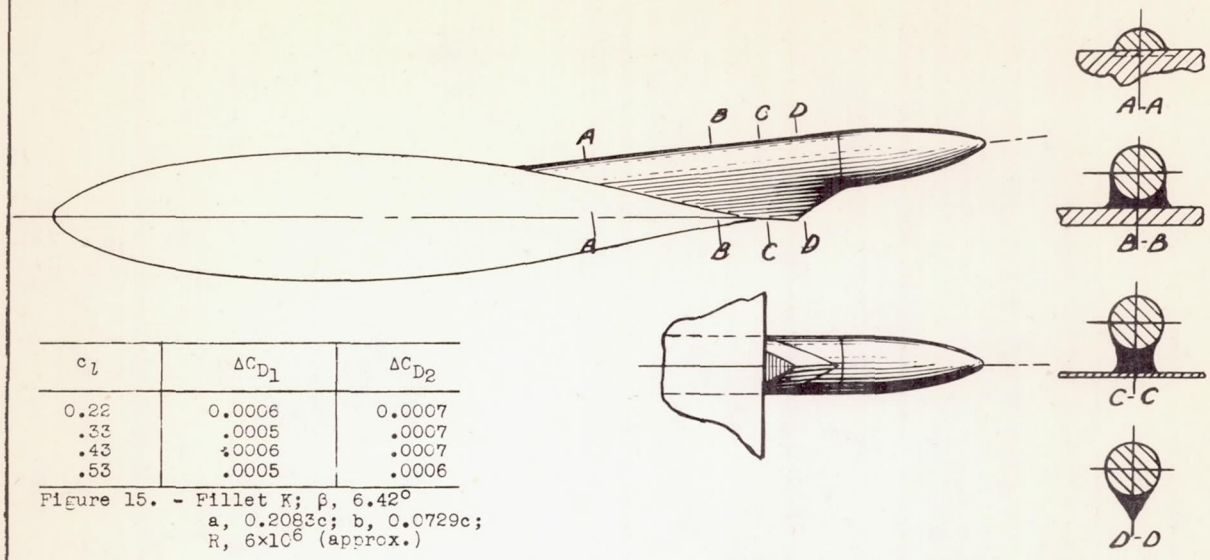

c_l	ΔC_{D_1}	ΔC_{D_2}
0.22	0.0006	0.0007
.33	.0005	.0007
.43	.0006	.0007
.53	.0005	.0006

Figure 15. - Fillet K; β, 6.42°
a, 0.2083c; b, 0.0729c;
R, 6×10^6 (approx.)

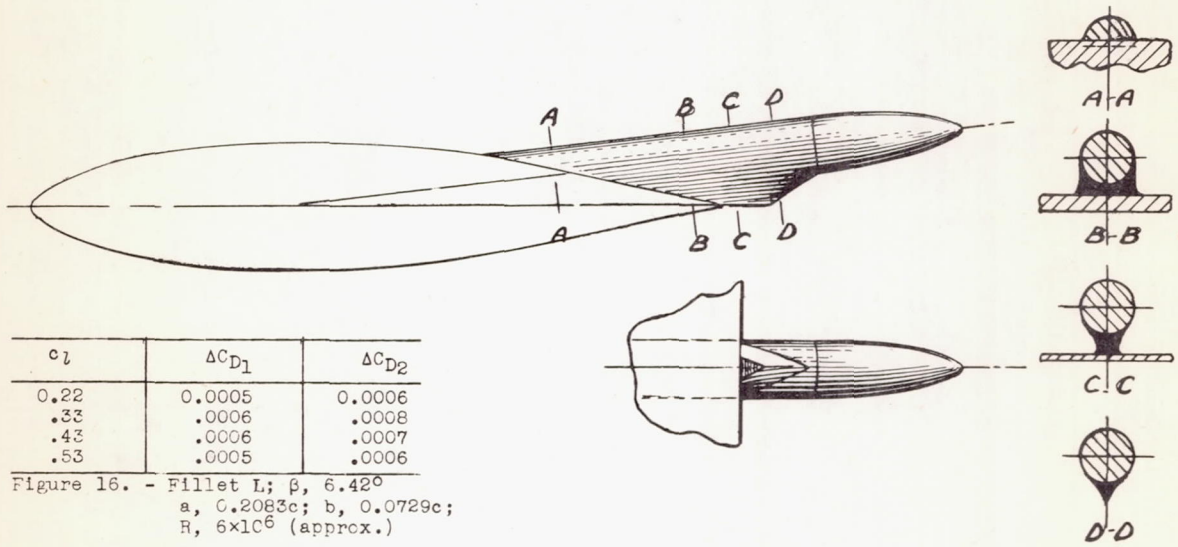

c_l	ΔC_{D_1}	ΔC_{D_2}
0.22	0.0005	0.0006
.33	.0006	.0008
.43	.0006	.0007
.53	.0005	.0006

Figure 16. - Fillet L; β, 6.42°
a, 0.2083c; b, 0.0729c;
R, 6×10^6 (approx.)

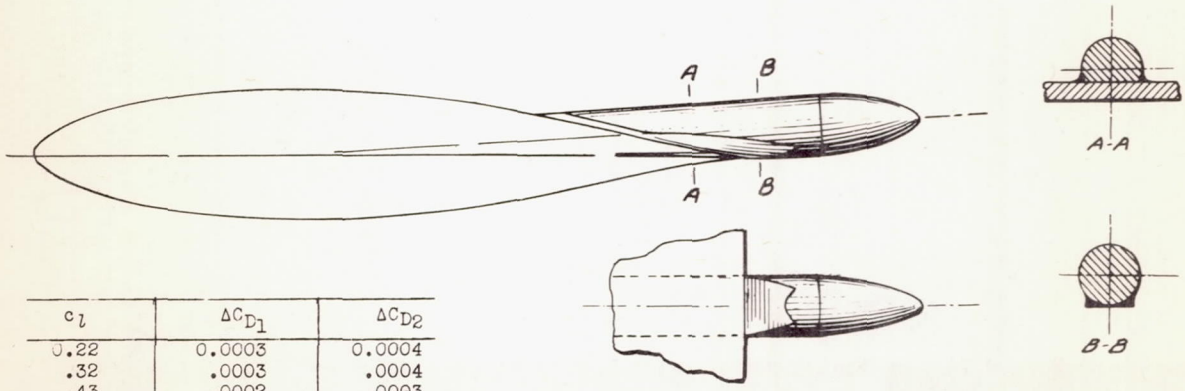

c_l	ΔC_{D_1}	ΔC_{D_2}
0.22	0.0003	0.0004
.32	.0003	.0004
.43	.0002	.0003
.53	.0003	.0004

Figure 17. - Fillet M; β, 3.25°
a, 0.1392c; b, 0.0729c;
R, 6×10^6 (approx.)

L-299

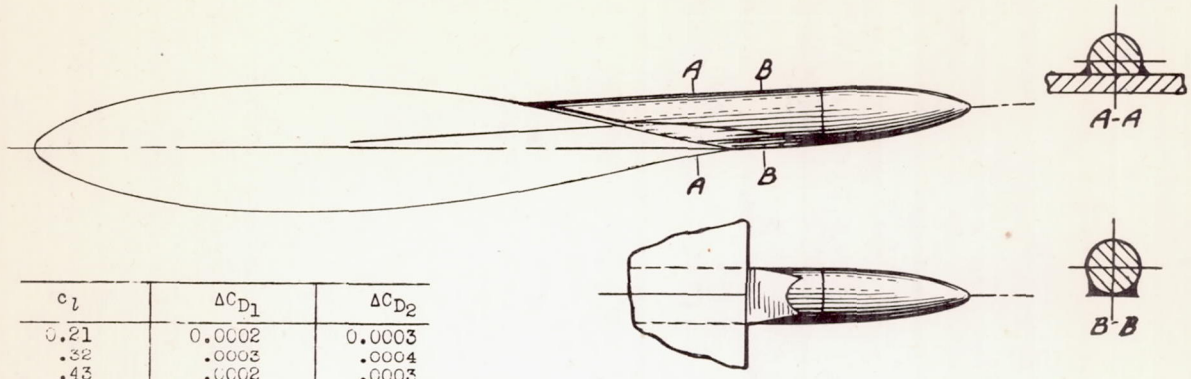

c_l	ΔC_{D_1}	ΔC_{D_2}
0.21	0.0002	0.0003
.32	.0003	.0004
.43	.0002	.0003
.53	.0004	.0004

Figure 18. - Fillet M; β, 3.25°
a, 0.2088c; b, 0.0729c;
R, 6×10^6 (approx.)

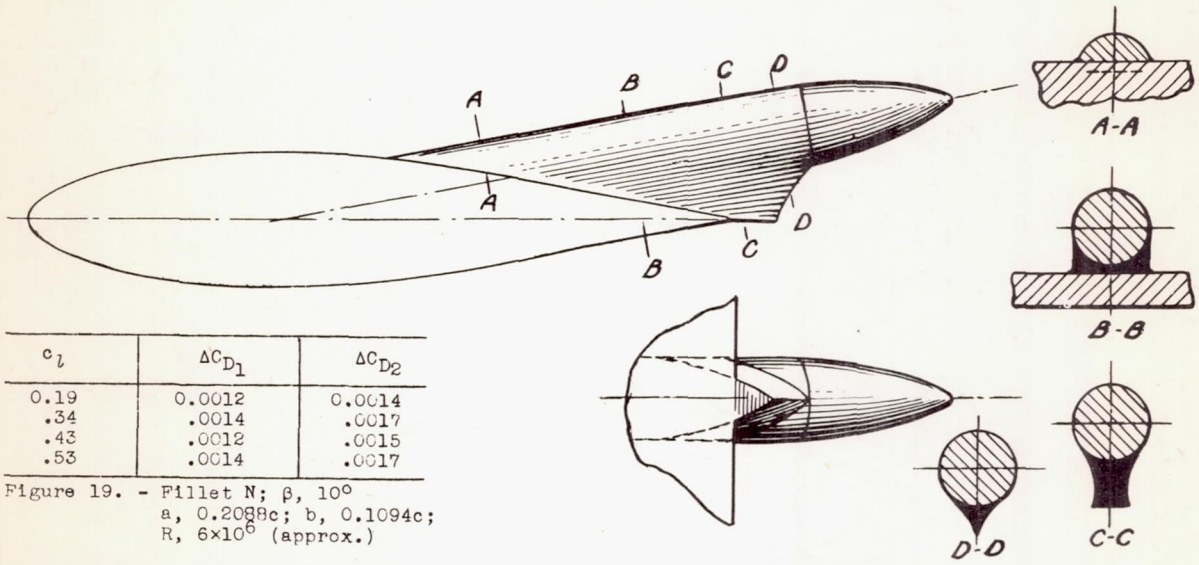

c_l	ΔC_{D_1}	ΔC_{D_2}
0.19	0.0012	0.0014
.34	.0014	.0017
.43	.0012	.0015
.53	.0014	.0017

Figure 19. - Fillet N; β, 10°
a, 0.2088c; b, 0.1094c;
R, 6×10^6 (approx.)

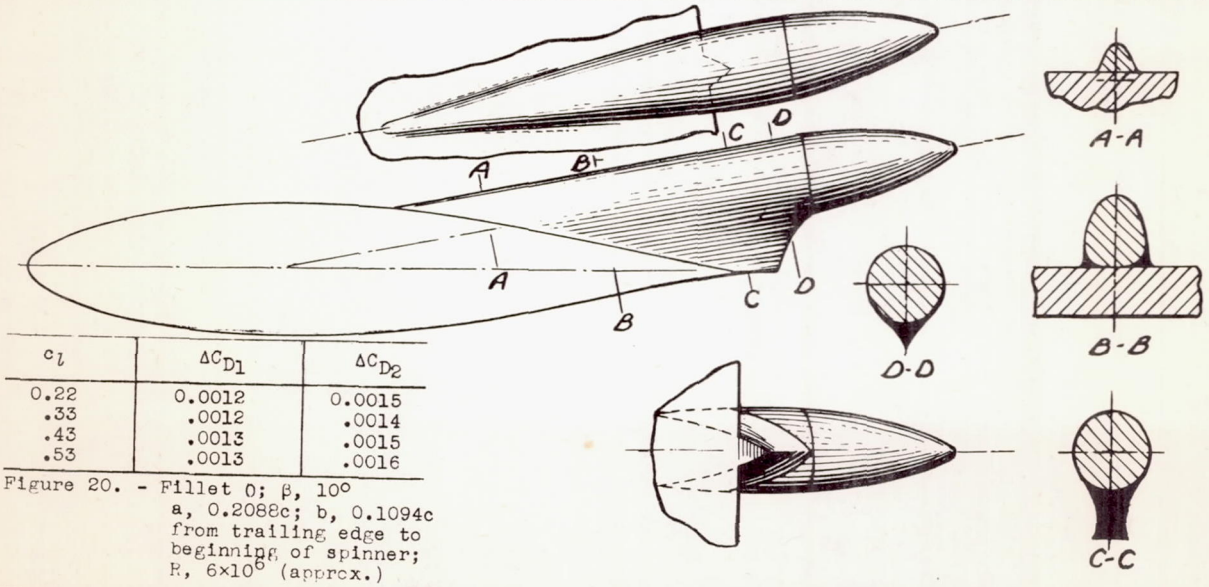

c_l	ΔC_{D_1}	ΔC_{D_2}
0.22	0.0012	0.0015
.33	.0012	.0014
.43	.0013	.0015
.53	.0013	.0016

Figure 20. - Fillet O; β, 10°
a, 0.2088c; b, 0.1094c
from trailing edge to
beginning of spinner;
R, 6×10^6 (approx.)

L-299

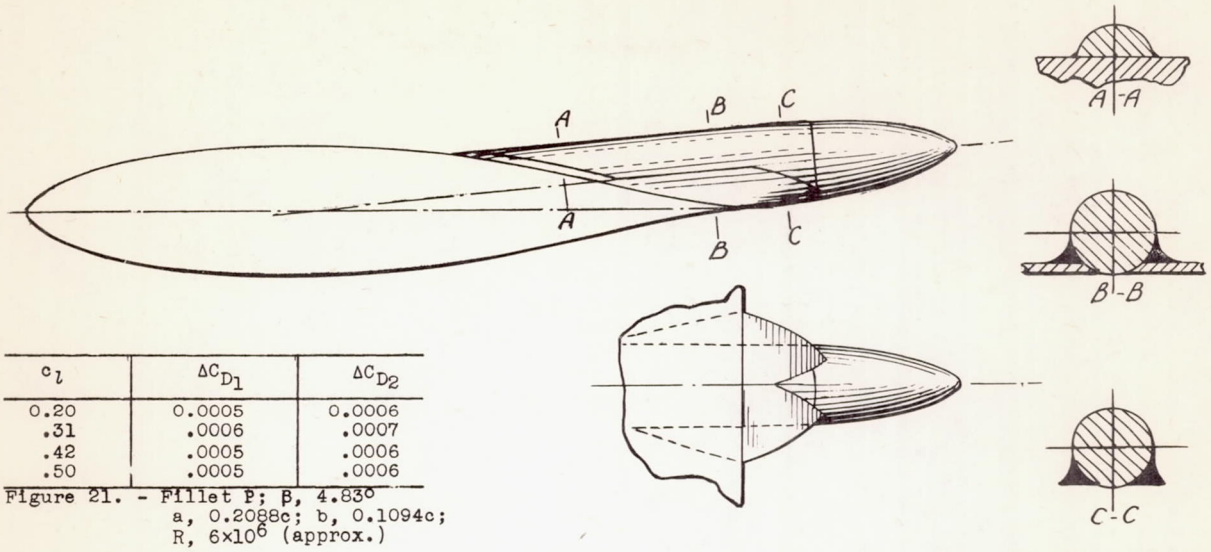

c_l	ΔC_{D_1}	ΔC_{D_2}
0.20	0.0005	0.0006
.31	.0006	.0007
.42	.0005	.0006
.50	.0005	.0006

Figure 21. - Fillet P; β, 4.83°
a, 0.2088c; b, 0.1094c;
R, 6×10^6 (approx.)

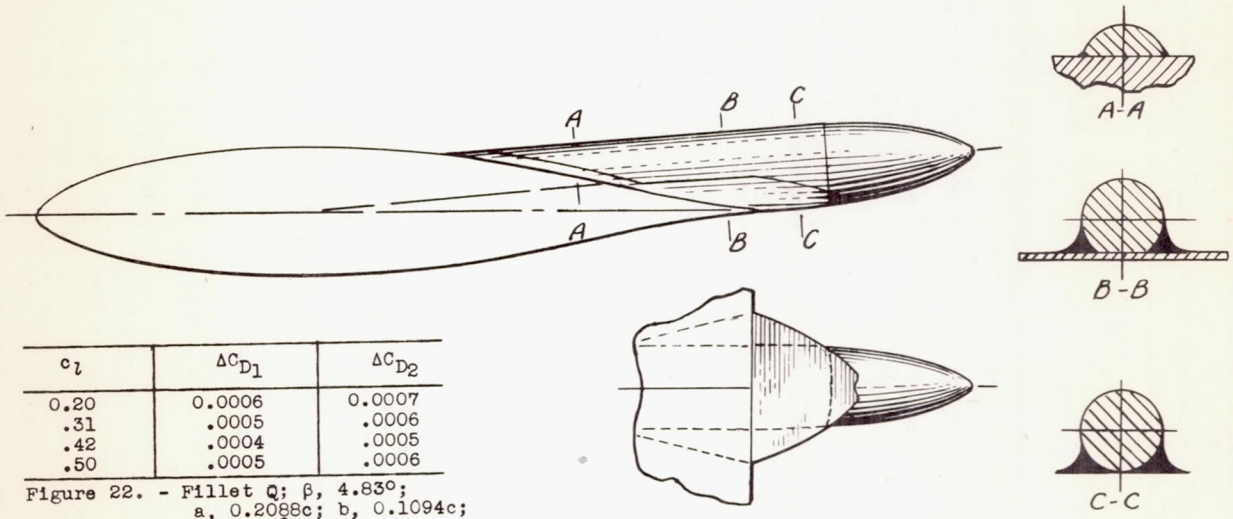

c_l	ΔC_{D_1}	ΔC_{D_2}
0.20	0.0006	0.0007
.31	.0005	.0006
.42	.0004	.0005
.50	.0005	.0006

Figure 22. - Fillet Q; β, 4.83°;
a, 0.2088c; b, 0.1094c;
R, 6×10^6 (approx.)

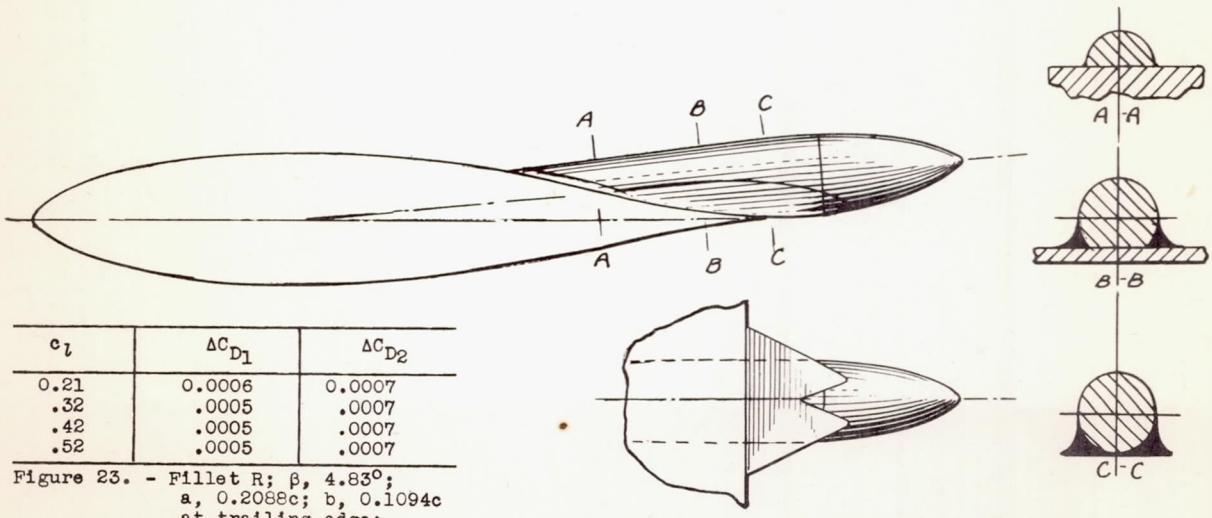

c_l	ΔC_{D_1}	ΔC_{D_2}
0.21	0.0006	0.0007
.32	.0005	.0007
.42	.0005	.0007
.52	.0005	.0007

Figure 23. - Fillet R; β, 4.83°;
a, 0.2088c; b, 0.1094c
at trailing edge;
R, 6×10^6 (approx.)

L-299

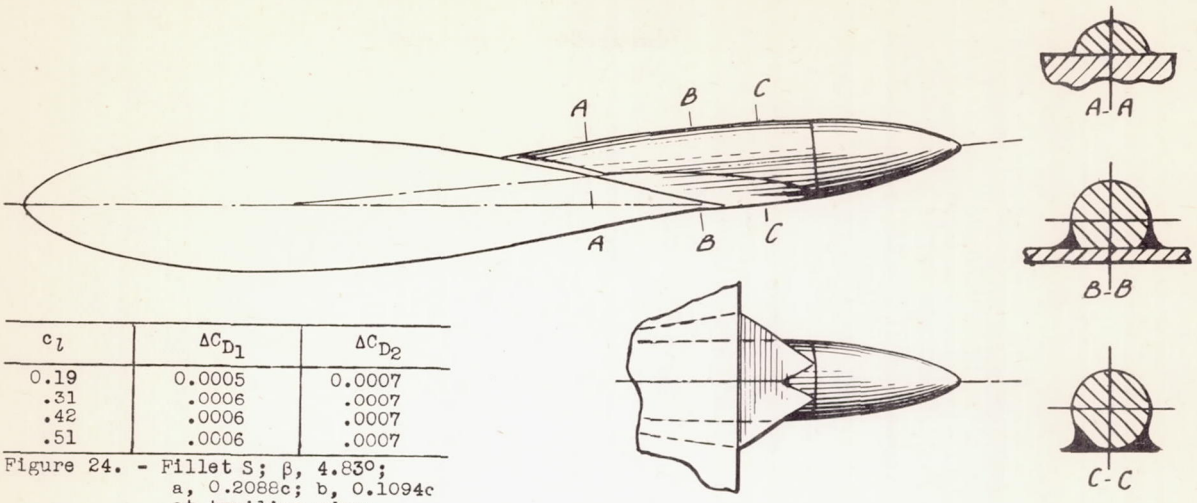

c_l	ΔC_{D_1}	ΔC_{D_2}
0.19	0.0005	0.0007
.31	.0006	.0007
.42	.0006	.0007
.51	.0006	.0007

Figure 24. - Fillet S; β, 4.83°; a, 0.2088c; b, 0.1094c at trailing edge; R, 6×10^6 (approx.)

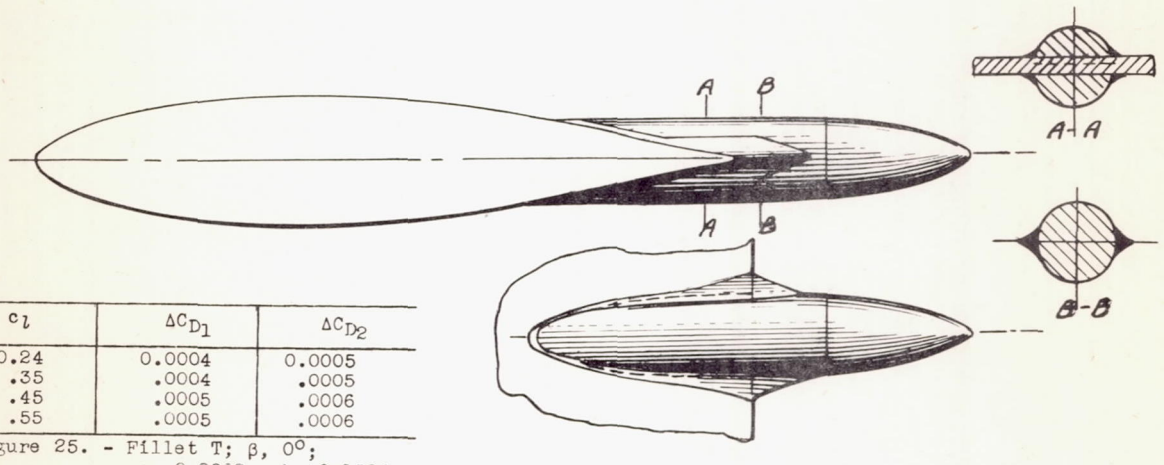

c_l	ΔC_{D_1}	ΔC_{D_2}
0.24	0.0004	0.0005
.35	.0004	.0005
.45	.0005	.0006
.55	.0005	.0006

Figure 25. - Fillet T; β, 0°; a, 0.2088c; b, 0.1094c; R, 6×10^6 (approx.)

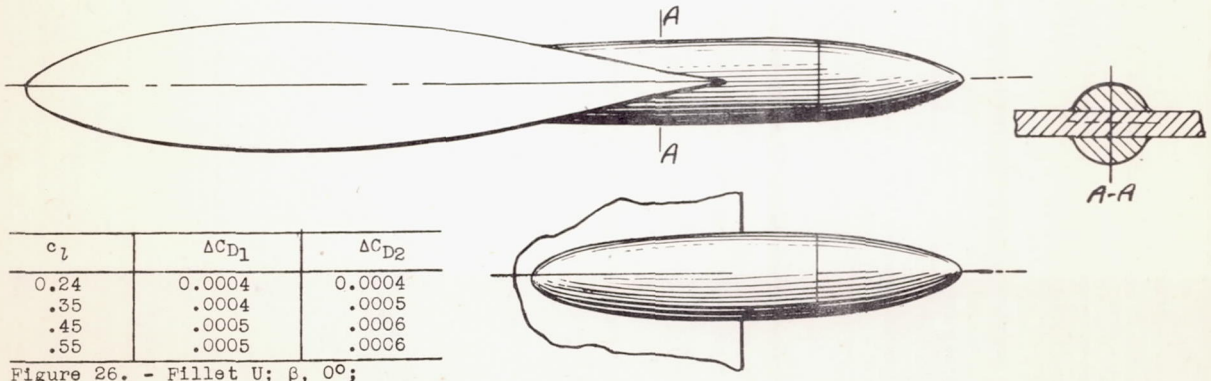

c_l	ΔC_{D_1}	ΔC_{D_2}
0.24	0.0004	0.0004
.35	.0004	.0005
.45	.0005	.0006
.55	.0005	.0006

Figure 26. - Fillet U; β, 0°; a, 0.2088c; b, 0.1094c; R, 6×10^6 (approx.)

L-299

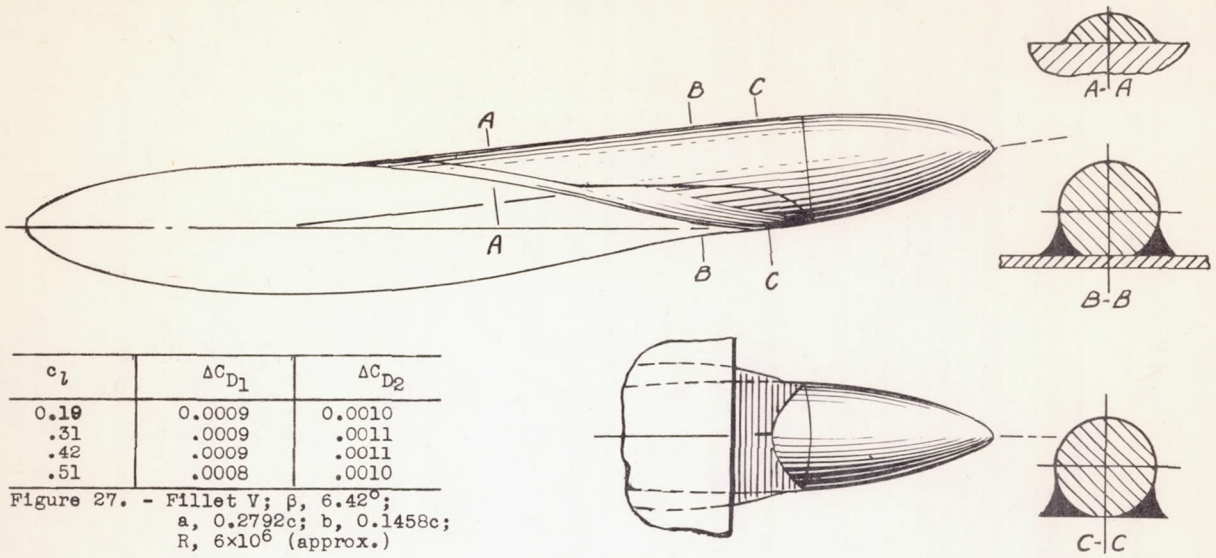

c_l	ΔC_{D_1}	ΔC_{D_2}
0.19	0.0009	0.0010
.31	.0009	.0011
.42	.0009	.0011
.51	.0008	.0010

Figure 27. - Fillet V; β, 6.42°; a, 0.2792c; b, 0.1458c; R, 6×10^6 (approx.)

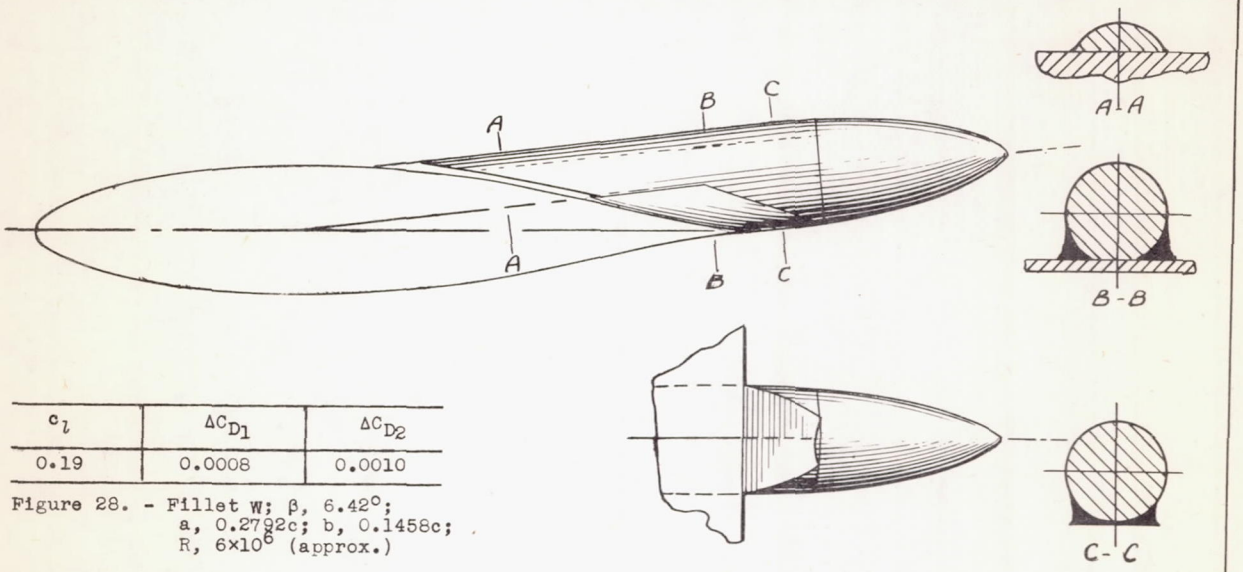

c_l	ΔC_{D_1}	ΔC_{D_2}
0.19	0.0008	0.0010

Figure 28. - Fillet W; β, 6.42°; a, 0.2792c; b, 0.1458c; R, 6×10^6 (approx.)

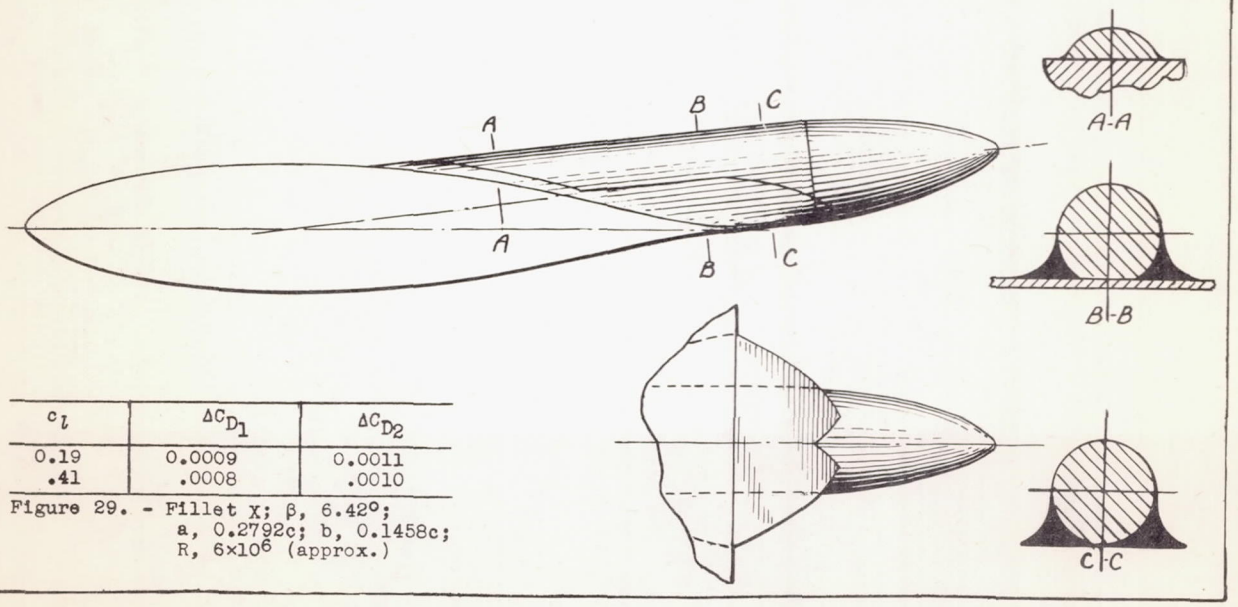

c_l	ΔC_{D_1}	ΔC_{D_2}
0.19	0.0009	0.0011
.41	.0008	.0010

Figure 29. - Fillet X; β, 6.42°; a, 0.2792c; b, 0.1458c; R, 6×10^6 (approx.)

L-299

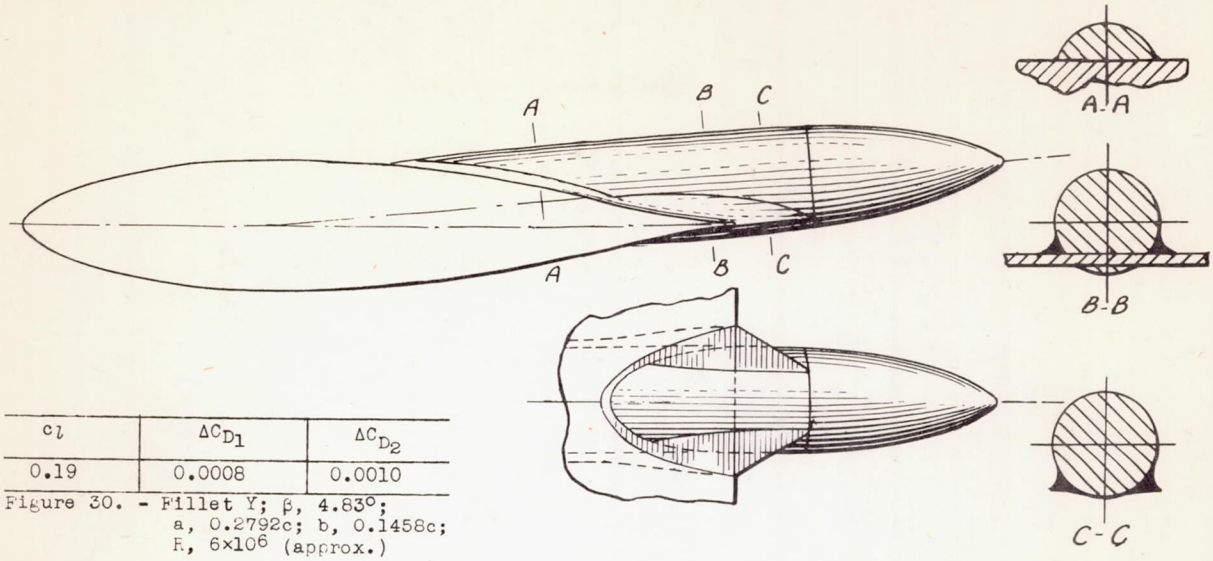

c_l	ΔC_{D_1}	ΔC_{D_2}
0.19	0.0008	0.0010

Figure 30. - Fillet Y; β, 4.83°;
a, 0.2792c; b, 0.1458c;
R, 6×10^6 (approx.)

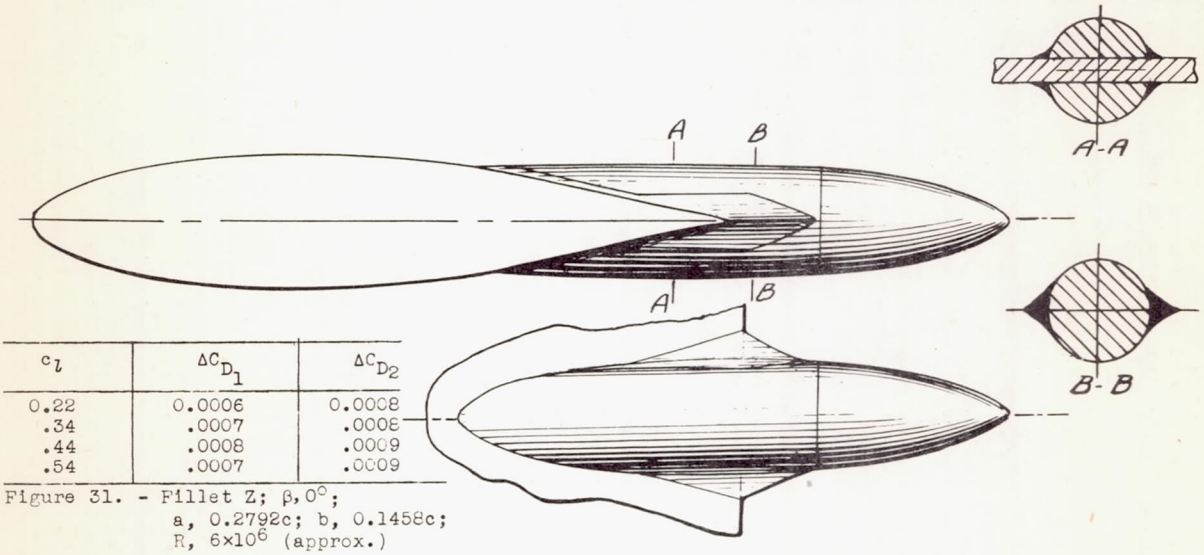

c_l	ΔC_{D_1}	ΔC_{D_2}
0.22	0.0006	0.0008
.34	.0007	.0008
.44	.0008	.0009
.54	.0007	.0009

Figure 31. - Fillet Z; β, 0°;
a, 0.2792c; b, 0.1458c;
R, 6×10^6 (approx.)

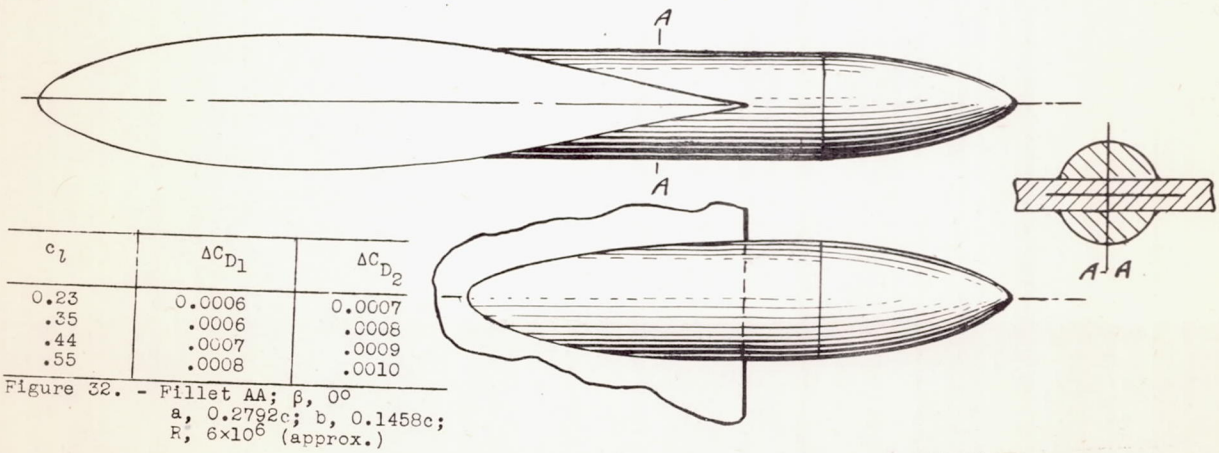

c_l	ΔC_{D_1}	ΔC_{D_2}
0.23	0.0006	0.0007
.35	.0006	.0008
.44	.0007	.0009
.55	.0008	.0010

Figure 32. - Fillet AA; β, 0°
a, 0.2792c; b, 0.1458c;
R, 6×10^6 (approx.)

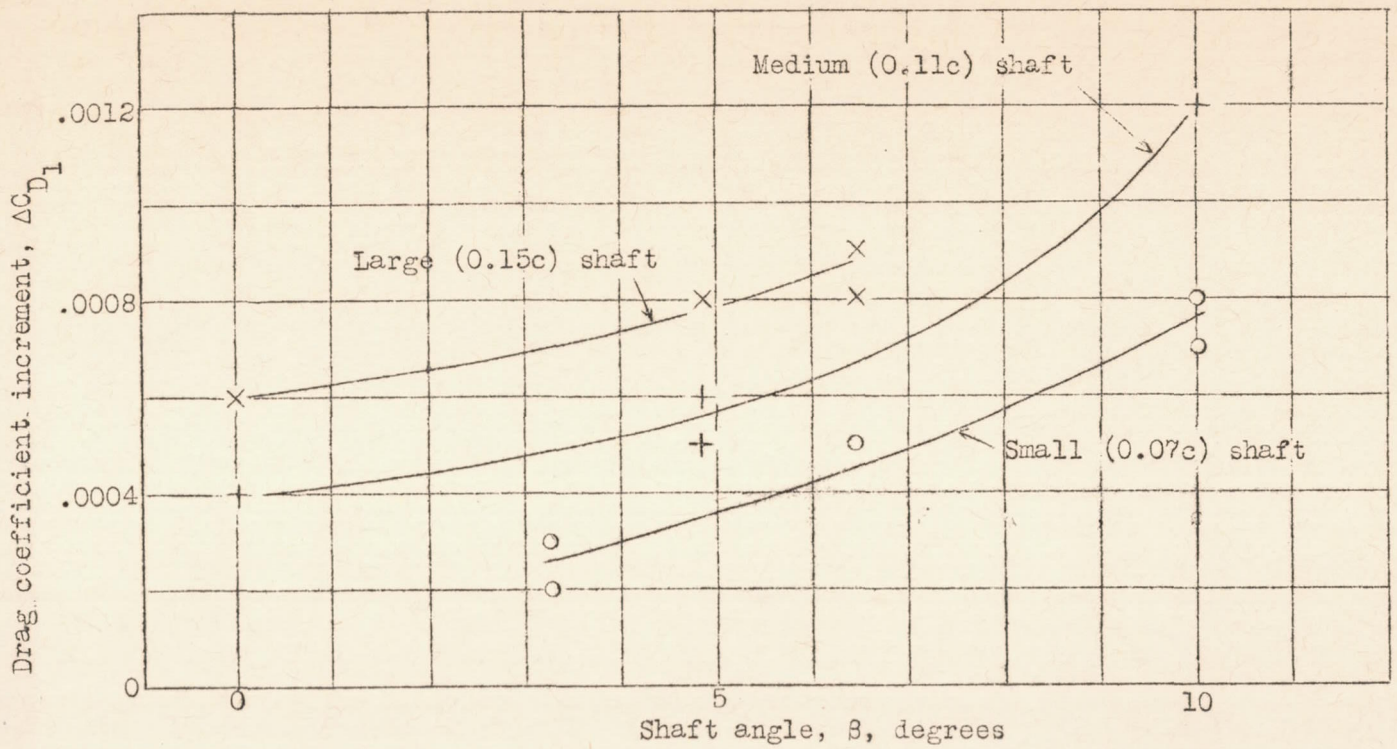

Figure 33.- The effect of shaft size and angularity on drag increments for pusher-propeller shaft combinations on an NACA 65,3-018 airfoil section; R, 6×10^6 (approximately).

L-299

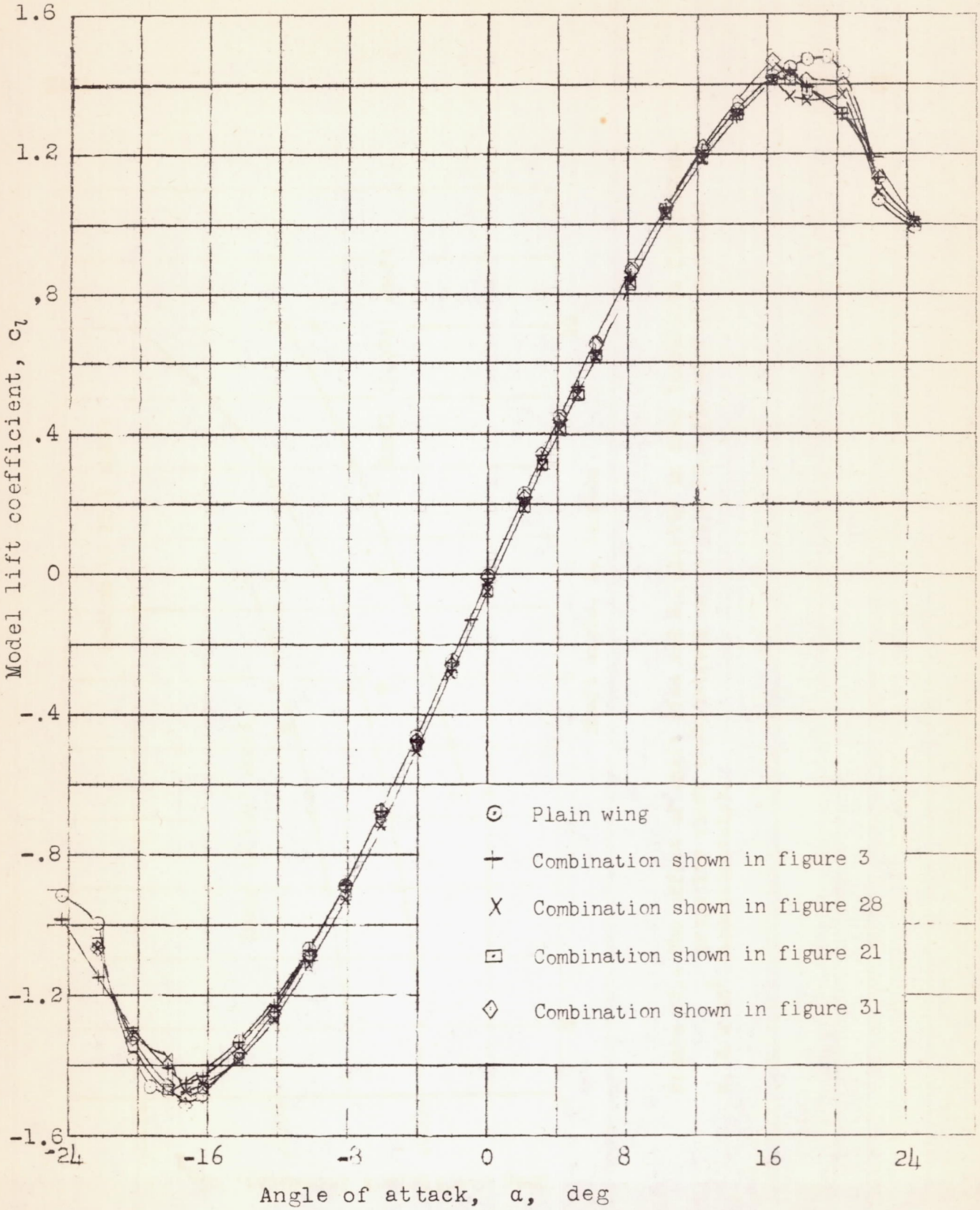

Figure 34.- Typical lift characteristics of NACA 65,3-018 airfoil section with pusher-propeller shaft combinations; R, 6×10^6 (approximately).